Translational Oncology
www.transonc.com

Volume 10 Number 6 December 2017 pp. 998–1007 998

Retrospective Proteomic Analysis of a Novel, Cancer Metastasis-Promoting RGD-Containing Peptide

Michiyo Tsuru[*,†,‡], Michio Sata[†,§], Maki Tanaka[¶], Hideaki Umeyama[#], Yoshio Kodera[**], Mieko Shiwa[††], Norikazu Aoyagi[††], Kaori Yasuda[‡‡], Kei Matsuoka[†,§§], Takaaki Fukuda[¶¶], Hideaki Yamana[†,##] and Kensei Nagata[*†,‡]

*Clinical Proteomics and Gene Therapy Laboratory, Kurume University, Kurume, Japan; [†]Research Center for Innovative Cancer Therapy, Kurume University, Kurume, Japan; [‡]Department of Orthopedic Surgery, Kurume University School of Medicine, Kurume, Japan; [§]Division of Gastroenterology, Department of Medicine, Kurume University School of Medicine, Kurume, Japan; [¶]Department of Surgery, Kurume General Hospital, Kurume, Japan; [#]Department of Biological Science, Chuo University, Tokyo, Japan; [**]Department of Physics, School of Science, Kitasato University, Kanagawa, Japan; [††]Life Science Division, Bio-Rad Laboratories K.K., Tokyo, Japan; [‡‡]Cell Innovator Co., Ltd., Fukuoka, Japan; [§§]Department of Urology, Kurume University, Kurume, Japan; [¶¶]Center for Rheumatology, Kurume University School of Medicine, Kurume, Japan; [##]Center for Multidisciplinary Treatment of Cancer, Kurume University School of Medicine, Kurume, Japan

Abstract

Patients who undergo surgical extirpation of a primary liver carcinoma followed by radiotherapy and chemotherapy leading to complete remission are nevertheless known to develop cancerous metastases 3–10 years later. We retrospectively examined the blood sera collected over 8 years from 30 patients who developed bone metastases after the complete remission of liver cancer to identify serum proteins showing differential expression compared to patients without remission. We detected a novel RGD (Arg-Gly-Asp)-containing peptide derived from the C-terminal portion of fibrinogen in the sera of metastatic patients that appeared to control the EMT (epithelial-mesenchymal transition) of cancer cells, in a process associated with miR-199a-3p. The RGD peptide enhanced new blood vessel growth and increased vascular endothelial growth factor levels when introduced into fertilized chicken eggs. The purpose of this study was to enable early detection of metastatic cancer cells using the novel RGD peptide as a biomarker, and thereby develop new drugs for the treatment of metastatic cancer.

Translational Oncology (2017) 10, 998–1007

Background

Liver cancer is the second leading cause of cancer-related deaths, and the fifth most common form of cancer worldwide [1]. It is most common in Asia, and hence is of particular concern in Japan. Liver cancer typically takes upward of 30 years to develop following infection with hepatitis C virus or other pathogens. In most Japanese cases, the incidence of disease can be linked to the country's hepatitis C outbreak in the years immediately following the Second World War [2–4]. This has led to the current epidemic of liver cancer among

Address all correspondence to: Michiyo Tsuru, Clinical Proteomics and Gene Therapy Laboratory, Research Center for Innovative Cancer Therapy, Kurume University, 67-Asahi-machi, Kurume, 830-0011, Japan.
E-mail: michiyo@med.kurume-u.ac.jp
Received 29 July 2017; Revised 2 October 2017; Accepted 5 October 2017

1936-5233/17
https://doi.org/10.1016/j.tranon.2017.10.001

Japanese adults who were in their teens, 20s, and 30s near the end of the war.

Early diagnoses and ongoing advances in treatment have led to improvements in the remission rates for cancers that are exclusively present within primary foci. However, advanced cancers with distant metastases still have very poor prognoses, with treatment often focusing more on palliative care and preventing further metastases than on the cancer therapy itself [5–7]. Cancer metastasis is facilitated by the production of vascular endothelial growth factor (VEGF) and angiogenesis, and causes the epithelial–mesenchymal transition (EMT), which leads to enhanced cell migration and infiltration. Controlling metastasis and understanding its pathology are therefore essential for eliminating cancer cells within the body.

In the present study, we conducted a retrospective proteomic analysis of the sera from 30 patients who had developed bone metastases after complete remission of liver cancer 8 years prior. We aimed to identify serum proteins that were differentially expressed between those patients with complete remission and those without.

Methods

Ethical Guidelines

The study protocol was approved by Kurume University Hospital (Approval Number 2547). An anonymous retrospective study was conducted, following Freezerworks validation procedures, as per US Food and Drug Administration guidelines, on 47 Japanese cancer patients during a follow-up period from 1994 to 2002 (see Supplemental Study Protocol). Before conducting an analysis of any patient serum samples, we obtained informed consent on the serum survey, including the use of all preserved blood for measurement in this study, and we also received written consent from other cancer patients and healthy volunteers. Patients started treatment after the diagnosis of metastasis was confirmed by the quantification of CFMP in serum and imaging diagnosis. Standard treatments were administered, which were not affected by the decision of the patient's participation in the study. Samples were collected using Venoject II 7-mL tubes equipped with a clot activator and gel separator (VP-P073K; Terumo, Tokyo, Japan), and the serum was then separated by centrifugation followed by preservation at −80 °C.

Animal Welfare and Management

Strain SHO SCID mice (Crlj:SHO-Prkdc^{scid} Hr^{hr}, 4 weeks old) were purchased from Charles River, Yokohama, Japan. Severity assessment in laboratory animals is an important issue with respect to implementing the 3Rs concept in biomedical research, and is a pivotal feature of current Japanese regulations [8]. All experiments were approved and permitted by Kurume University. Chicken eggs and the SCID mice were monitored daily for health and weight. All procedures, including the euthanasia of morbidly ill mice and chicken embryos, were performed under isoflurane (minimum alveolar concentration at approximately 50% atm; MAC_{50}, 1.41%) and ketamine anesthesia (80 mg/kg) according to standard protocols and the Guidelines for Proper Conduct of Animal Experiments (Science Council of Japan) [9]. On the basis of the pain classification of the Scientists Center for Animal Welfare (SCAW), tumor diameters >20 mm and high levels of cancer markers were defined as humane endpoints and noninvasive imaging analysis was performed (narcotics handler license: 230,263/2011–2012, 250,263/2013–2014, 270,263/2015–2016, 170,263/2017) [10]. The procedures were conducted in accordance with the Law Concerning the Conservation and Sustainable Use of Biological Diversity through Regulations on the Use of Living Modified Organisms; the protocol was approved under Type 2 Regulations Concerning the Use of Living Modified Organisms of Kurume University (approval no. 22–7) and was carried out following International Council for Laboratory Animal Science (ICLAS) approval (approval nos. 18–2/2010, 43/2011, 190/2012, 165/2013, 54–1/2014, 20/2015 45/2016 and 136/2017) [11,12]. Routine microbiologic monitoring according to recommendations of the Federation of ICLAS did not reveal any evidence of infection with common urine pathogens [13]. The SCID mice were maintained in specific-pathogen-free (SPF) Level P1A rooms with a controlled environment: 21 ± 2 °C; relative humidity 55 ± 5%; 12:12 h light:dark cycle (lights on at 7:00 a.m.), with 12–14 air changes hourly. Pelleted diet (CE-2, CLEA, Japan) and autoclaved (135 °C/60 min) distilled water were provided *ad libitum*. There were no significant adverse events noted in the SCID mice experiments.

Cell Lines

The human non-small cell lung cancer cell line H460, the breast cancer cell line BT474, the bone metastatic prostate cell line PC-3, and the osteosarcoma MNNG/HOS cell line were purchased from the American Type Culture Collection (ATCC) (Manassas, VA, USA). H460-GFP, osteosarcoma HNNG/HOS-GFP, BT474-GFP, and PC3-GFP cell lines were purchased from AntiCancer Inc. (San Diego, CA, USA). HMVEC-L; human lung microvascular endothelial cells) and mesenchymal stem cells purchased from Lonza Inc. (Basel, Switzerland).

Design

We carried out a proteomics analysis to identify serum proteins that are differentially expressed between liver cancer patients who had complete remission and those who did not. Our sample set was composed of 47 Japanese patients (25 men, 22 women; mean age: 55 years; age range: 52–68 years), of which 30 (17 men, 13 women; mean age: 61 years; age range: 21–60 years) developed bone metastasis in 2002, following complete remission in 1994. Bone metastases for each patient were confirmed using positron emission tomography-computed tomography (PET-CT) as part of the patients' standard of care. In order to investigate the effect on racial differences, we also obtained serum from Analytical Biological Services Inc. (Wilmington, DE, USA). The sera were obtained from five Caucasian females (39–66 years old) who had breast cancer with bone metastasis, with infiltrating ductal carcinoma or infiltrating lobular carcinoma, based on their histological diagnosis (Supplemental Carcinoma Data). As controls, we also examined the serum proteins from two groups of adult volunteers (1) 21 healthy controls (9 men, 12 women; mean age: 51 years; age range: 21–60 years) with no malignant tumors identified during health check-ups or by PET-CT, and (2) 17 patients with rheumatoid arthritis (2 men, 15 women; mean age: 54 years; age range: 43–63 years, American College of Rheumatology; ACR, class I; 4, class II; 4, class III; 4, and class IV; 5 (https://www.rheumatology.org/Practice-Quality/Clinical-Support/Clinical-Practice-Guidelines) (Supplemental Study Protocol).

For patients who developed bone metastasis later on, this occurred after complete remission of their liver cancer *via* surgical extirpation of a primary carcinoma followed by radiotherapy and chemotherapy.

We had previously performed a proteomic analysis of their sera obtained as early as 1994, a full 8 years prior to the occurrence of bone metastasis. For these patients, complete remission was defined according to tumor guidelines [14], using low values of tumor markers and diagnostic imaging as indicators. We also performed a similar investigation for seven patients with breast cancer who expressed the novel RGD-containing peptide, described later, after complete remission following radiation treatment and chemotherapy.

Among the 47 patients with complete remission of liver cancer, 30 patients who developed bone metastases and 17 patients, who did not develop bone metastases, were retrospectively investigated. Healthy individuals and patients with rheumatoid arthritis were examined as controls and after the amino acid sequence of the peptide was identified, metastases other than bone metastasis, were investigated.

Targeting Proteomics

Traditional discovery proteomics [15] using modern Surface-enhanced laser desorption ionization time-of-flight mass spectrometry (SELDI-TOF-MS) [16,17] (as previously described) usually progresses directly to the clinical validation stage where large cohorts of patients are evaluated using well-established, validated methodologies (such as enzyme-linked immunosorbent assays (ELISAs) prior to clinical implementation [18]. For SELDI, a weak cation exchange chip (CM10), a strong cation exchange chip (Q10), a copper modified chip (IMAC30), and a negative-phase chip (H50) were used. For catenation and wash buffers, 100 mM sodium acetate (pH 4) and 50 mM HEPES (pH 7) were used for CM10, 50 mM Tris–HCl (pH 8) and 100 mM sodium acetate (pH 5) were used for Q10, 100 mM sodium phosphate +0.5 M NaCl (pH 7) was used for IMAC30, and 50 mM HEPES (pH 7) was used for H50. First, after adding 100 mM $CuSO_4$ to the IMAC30 chip and shaking for 10 minutes, the chip was washed with ultra-pure water (twice, 2 minutes/wash) and copper was fixed onto the chip's surface. After adding 0.1 M sodium acetate (pH 4) and shaking for 5 minutes, the chip was washed for 2 minutes with ultra-pure water. The four types of chips were then catenated and washed with a wash buffer (twice, five minutes/wash), and the chip surfaces were equalized. Following this, 100 μL of a five-fold dilution of the sample and wash buffer was added and the chip was shaken for 30 minutes. After adding the catenation and wash buffer, shaking, and washing the chip surface (three times, 5 minutes/wash), desalination was performed using ultra-pure water. After air-drying the chip, 2 μL of a 50% saturated solution of sinapinic acid was added and air-dried (twice). In addition, porcine dynorphin (2147.5 m/z), human ACTH (1–24) (2933.5 m/z), bovine insulin (β-chain) (3495.9 m/z), human insulin (5807.7 m/z), recombinant hirdin (6963.5 m/z), hirdin BHVK (7033.6 m/z), bovine cytochrome C (12,230.9 m/z), equine myoglobin (16,951 m/z), bovine carbonic anhydrase (29,023 m/z), and *S. cerevisiae* enolase (46,671 m/z) were used as molecular weight calibration proteins.

The protein chips were measured using the protein chip reader PCS4000 (Bio-Rad) and data was obtained through CiphergenExpress™ Data Manager version 3.0 (Bio-Rad). The measurement ranges were 0–100,000 m/z (Focus mass/SPA-Low; 6500) as the low molecular field data and 10,000–200,000 m/z (Focus mass/SPA-High; 20,000) as the high molecular field data. All measurements were performed in duplicate. Data analysis was performed using CiphergenExpress™ Data Manager version 3.0. After baseline correction of the measured spectra, normalization was conducted between the spectra by means of molecular weight calibration and normalization. The peak of the analysis target was a signal/noise (s/n) ratio >2.5. In regards to the relative expression intensity for the peaks in cancerous and non-cancerous areas, a significance test was performed using a Mann–Whitney *U* test, and a *P* value below .05 was determined to be a significant difference. In addition, a Receiver Operating Characteristic (ROC) plot was done, the area under curve was calculated, and a single marker analysis was assessed.

Results

Protein Identification and Characterization

Of the47 patients with primary liver cancer who achieved remission, we conducted a retrospective proteomic analysis of the sera from 30 patients who developed bone metastasis over 8 years. Purified fractions from HPLC were analyzed by TOF-MS, which revealed a target peak of interest in the range of m/z 2000–100,000. LC–MS/MS analysis narrowed the location of the peak of interest down to m/z 5813. We named the 5813 Da peptide circulating fibrinogen metastatic peptide (referred to hereinafter as CFMP, a 41-aa peptide). The peak at MW 5813 was detected before the onset of bone metastasis in all patients, and its levels increased over time. Expression of CFMP peaked at the time of the definitive diagnosis of bone metastases by bone scintigraphy, and decreased after the start of subsequent chemotherapy and radiation treatment (Figure 1, *A* and *B*). No expression was detected in the serum of healthy controls or patients with rheumatoid arthritis (Figure S1*A*). The peptide was an RGD-containing peptide comprising 41 amino acids (CQFTSSTSYNRGDSTFESKSYKMADEAGSEADHEGTHSTKR) (which corresponds to FGA amino acids 582–621). Immunohistochemical staining demonstrated that both cancer cells and CFMP were detected in the blood vessels of human chondroblastic osteosarcoma tissue (Figure 1*C*) derived from a 13-year-old boy. *In situ* hybridization for CFMP revealed that it was expressed in numerous cancer tissues in patients, as well as in the liver of healthy individuals (Figure 1*D*).

Functional Characteristics of CFMP

In order to investigate whether CFMP has a role in the formation of new blood vessels, as one of the characteristics in cancer metastasis, we injected either water or a synthetic CFMP peptide into fertilized chicken eggs, and allowed the eggs to hatch in an incubator for 20 days, with egg rotation every 8 hours. We then obtained the vascular tissue surrounding the embryos before hatching (Figure 1*E*) in order to examine the presence of neo-vessels and measure the VEGF levels (Figure 1*F*). Significantly more new blood vessels were observed surrounding the twenty embryos injected with CFMP compared with those surrounding the five control embryos ($P < .001$).

H460 cells were cultured with CFMP along with normal human lung microvascular endothelial cells, or mesenchymal stem cells, on membranes containing 8.0-μm pores (Figure 2*A*). After 24 h of incubation, scanning electron microscopy showed that the cancer cells in the lower layer had migrated upward through the 8.0-μm pores but only when the upper layer contained mesenchymal stem cells, but not when it contained normal human lung microvascular epithelial cells (Figure 2*B*). RNA was extracted from the gel shown in Figure 2*A* and real time PCR was performed to examine the expression of GATA-2, with the data showing a high level of GATA-2 expression [19] (Figure S2*C*). MMP-13 (collagenase 3) is produced by breast cancer cells and chondrocytes [20–22]. It plays an important role in normal remodeling of bones and pathological

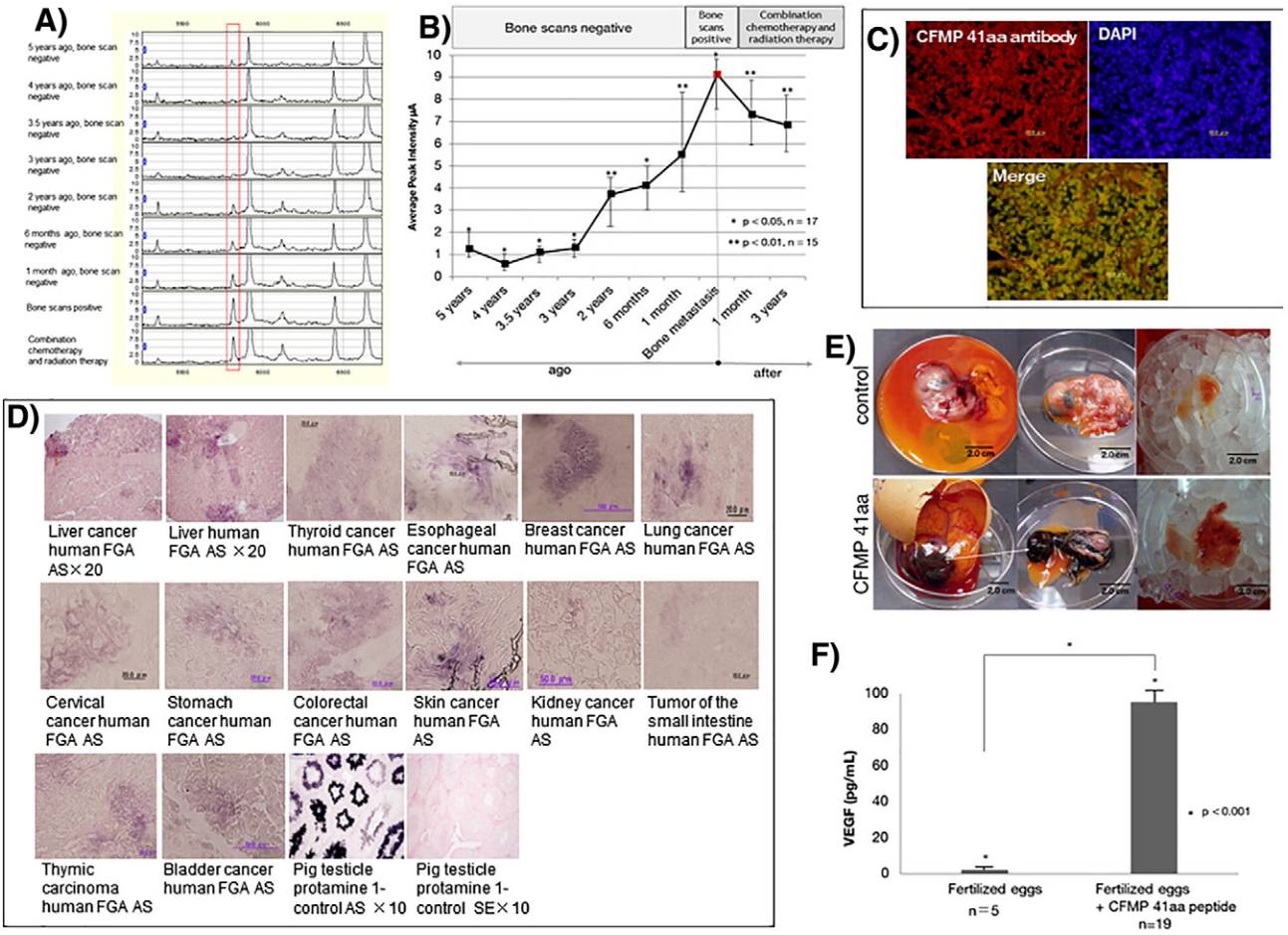

Figure 1. Discovery of the cancer metastasis-specific peptide. (**A**) Representative SELDI spectrum of serum from a cancer patient. (**B**) Time course of serum proteomics in patients who developed bone metastasis after the initial successful treatment of liver cancer. (**C**) Immunohistochemical detection of circulating fibrinogen metastatic peptide (CFMP, 41 aa) in the distal femur bone tumors from a 13-year-old boy. The anti-CFMP antibody was detected using an Alexa Fluor 555-labeled anti-rabbit secondary antibody. DAPI staining was also performed on tissue samples. CFMP was detected in cancer cells in the mesh. (**D**) *In situ* hybridization of CFMP mRNAs in primary cancer tissues. The expression of target mRNAs was confirmed in cancer tissues from the liver, lung, breast, skin, stomach, and kidney. Figure 1*D* shows the layout of the Multiple Tumor Tissue Array. (**E**) CFMP promotes cancer metastasis and participates in new blood vessel formation. A small, sterile hole was opened in a fertilized chicken egg, then water as a control or CFMP was injected. Dense new blood vessels formed around the embryo, suggesting that CFMP induces vascularization. Numerous new blood vessels were evident around the embryos, with significantly more vascular tissue in the embryos injected with the peptide (1.55 g, n = 20) than in untreated embryos (0.29 g, n = 5) ($P < .001$). (**F**) A VEGF ELISA of blood vessel tissues around the embryo also showed that CFMP induced neovascularization.

bone resorption, and its expression level is known to be regulated by the parathyroid hormone (PTH), retinoic acid and insulin-like growth factors. RNA was also isolated from the blood of healthy individuals as well as from breast cancer patients, and samples with a relative integrity number (RIN) of 8.3 were subjected to qRT-PCR analysis to measure *GATA2* and *MMP-13* levels, each of which is highly expressed in cancer metastasis. As a result, breast cancer patients were found to exhibit lower *GATA2* levels compared with control individuals (Figure 2*C*).

As mentioned previously, we synthesized a peptide encompassing the 576–628 aa region of FGA. The CFMP was removed and the amino acid sequence without the coiled-coil secondary structure was used as a negative control peptide to which we raised antibodies (15-aa antibody).

As mentioned previously, we synthesized a peptide encompassing the 576–628 aa region of FGA and as a negative control except FGA576–628 aa chain 15-aa peptides containing this region, to prepare 15-aa antibodies. Breast cancer BT474-GFP cells (AntiCancer Inc., San Diego, CA) stably expressing GFP and the labeled 15-aa negative peptide, comprising a sequence distinct from that of CFMP (HyLyte Fluor 555 C2 maleimide-CYGTGSETESPRNPSS) (FGA amino acid sequence 277–291 aa), were injected into nine female SCID SHO mice *via* the tail vein. We then examined the localization of the CFMP peptide in mouse tissues by fluorescent imaging, and Optix MX2 images were obtained at both 24 hours and 4 days after injection (Figures 3*A*, and S3*F*). After 4 days, fluorescence appeared in the cranial region. After 10 days, the entire body was fluorescent, and enhanced cancer marker visibility using an Optix MX2 Imager (ART Advanced Research Technologies, Inc., Montreal, Canada) was observed. Fourteen days after the CFMP peptide was introduced into the mouse, we confirmed that the tumors occurred in the head and neck area, and we observed the formation of neo-vascular vessels and bone tissues in the tumors using a 3D–CT analysis (Figure 3*B*). The

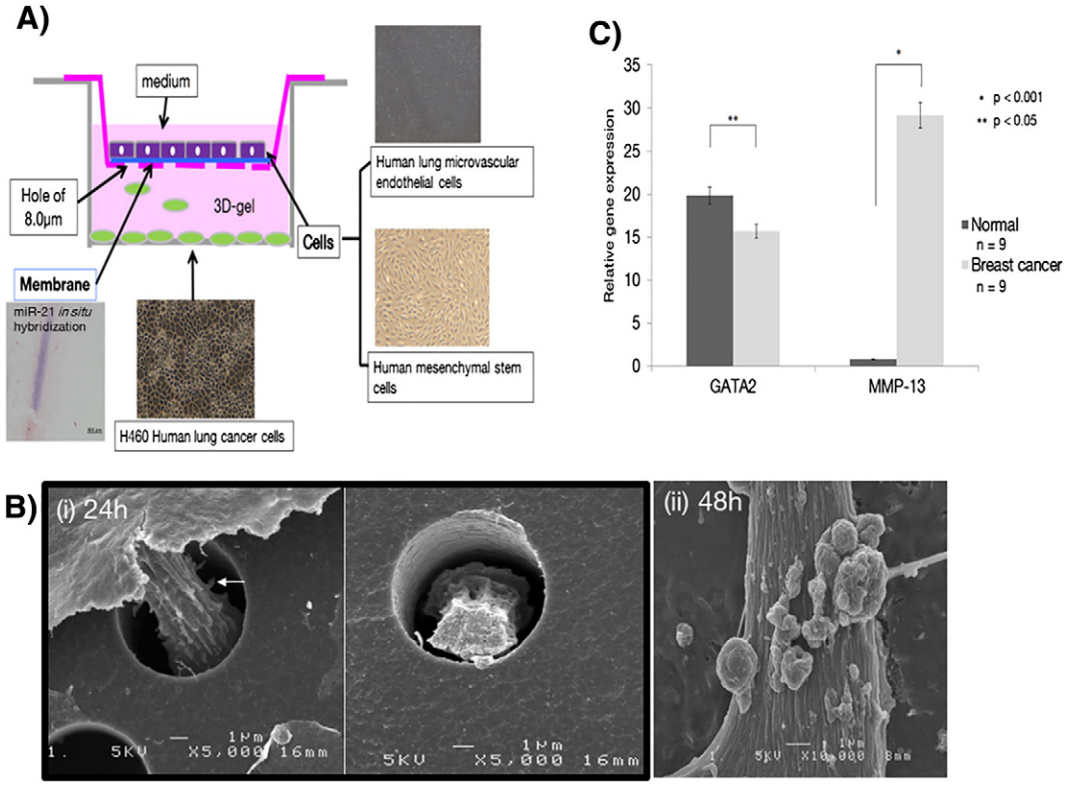

Figure 2. *In vitro* model of cancer metastasis. (**A**) Regulation of CFMP during the EMT. We investigated the motility of cancer cells *in vitro* using an adsorption assay which used miRNA array analysis. (**B**) Electron microscopic observation was performed on the mesenchymal stem cells in the upper part of the membrane in Figure 2*A*. (**i**) After 24 h, the membrane was observed by scanning electron microscopy (JSM-6320F; JEOL Ltd.; Tokyo, Japan). Normal human lung microvascular epithelial cells did not promote motility in the cancer cells, whereas pronounced motility was evident in the presence of normal human mesenchymal cells, with a large amount of tissue adhering around the cancer cells that had ascended the membrane. (**ii**) After 48 h, blood components, including platelets, had become deposited around the cancer tissue that had migrated upwards on the membrane. Scanning electron microscopic photography based on arrow aspect (**i**). (**C**) RNA was isolated from the blood of healthy individuals and breast cancer patients, and samples with an RIN of 8.3 were subjected to qRT-PCR analysis to determine the expression of GATA2 and MMP-13. Breast cancer patients exhibited lower GATA2 levels compared to healthy individuals. However, MMP-13 levels were higher in breast cancer patients.

tumors were confirmed to be adenocarcinoma by hematoxylin and eosin staining. Similar data were seen in all nine of the mice examined (Figure 3*C*).

We created thin-slices of tissues taken from the entire mouse 10 days after CFMP injection (5 μg/mL; 20 μL/g) (Figure 3*A* and Supplemental Methods), and examined these tissues for GFP-tagged cancer cells and the CFMP peptide using laser microscopy (Figure S3*F*). As shown in Figure 3*D*, whole body preparations of mice injected with BT474-GFP breast cancer cells and the CFMP peptide in Figure 3*A* were prepared and examined for the expression of GFP and Fluor 594-tagged CFMP using confocal laser microscopy. In breast cancer patients, metastasis typically occurs a long period of time (5 to 10 years) after chemotherapy or radiotherapy, and the reason for this delay is thought to be due to the fact that cancer cells can lie dormant in tissues. The aim of this analysis was to identify the tissues in which cancer cells and the CFMP peptide co-exist. As a result of this experiment, we discovered that the BT474-GFP breast cancer cells and the CFMP peptide were present in the same vascular tissue (Figure 3*D*).

Because miR-21 has previously been shown to be associated with cancer cell development [23–25], we performed *in situ* hybridization of miR-21 and observed its expression in vascular tissue (Figure 3*E*). Since there was no probe capable of quantitating the C-terminal region of FGA, we designed multiple primers capable of quantitating the CFMP nucleotide sequence. Two sets of primers were designed representing sequences inside and outside the sequence encoding CFMP. These primers are referred to FGA inner and FGA outer. FGA inner FW 5′-GTTCTCATCACCCTGGGATAGC-3′, FGA inner RV 5′-AGCTCTTGCTTTCAAATGTGGAG-3′, FGA outer FW 5′-TGGCATCTTCACAAATACAAAGG-3′, FGA outer RV 5′-ACTTAGTCTAGGGGGACAGGGAAG-3′ (Figure 3*F*) to detect FGA in the vascular tissues in the cancer metastasis model, as well as vascular tissues in the same model.

The two primer PCR assay indicated that there was a lower CFMP peptide level in an anti-CFMP antibody-administered mouse. mRNA was extracted from the blood of control mice or from the cancer metastasis model mice that had been administered antibodies against CFMP (Figure 3*G*), and subjected to qRT-PCR to measure the expression of the C-terminal FGA CFMP nucleotide sequence using the primers shown in Figure 3*F*. When anti-CFMP antibodies (7 mg/kg) were administered, the expression of CFMP, as well as the tumor incidence was suppressed (Figure 3*J*). Each tissue excised from the mouse cancer metastasis model was subjected to western blotting using antibodies to CFMP, integrin β3, p21, VEGF, and β-actin (Figure 3*H*).

Next, BT474 cells, with or without CFMP, were transplanted into mice. Metastasized head and neck tissues were excised and used to determine the relative expression levels of FGA, miR-21, and

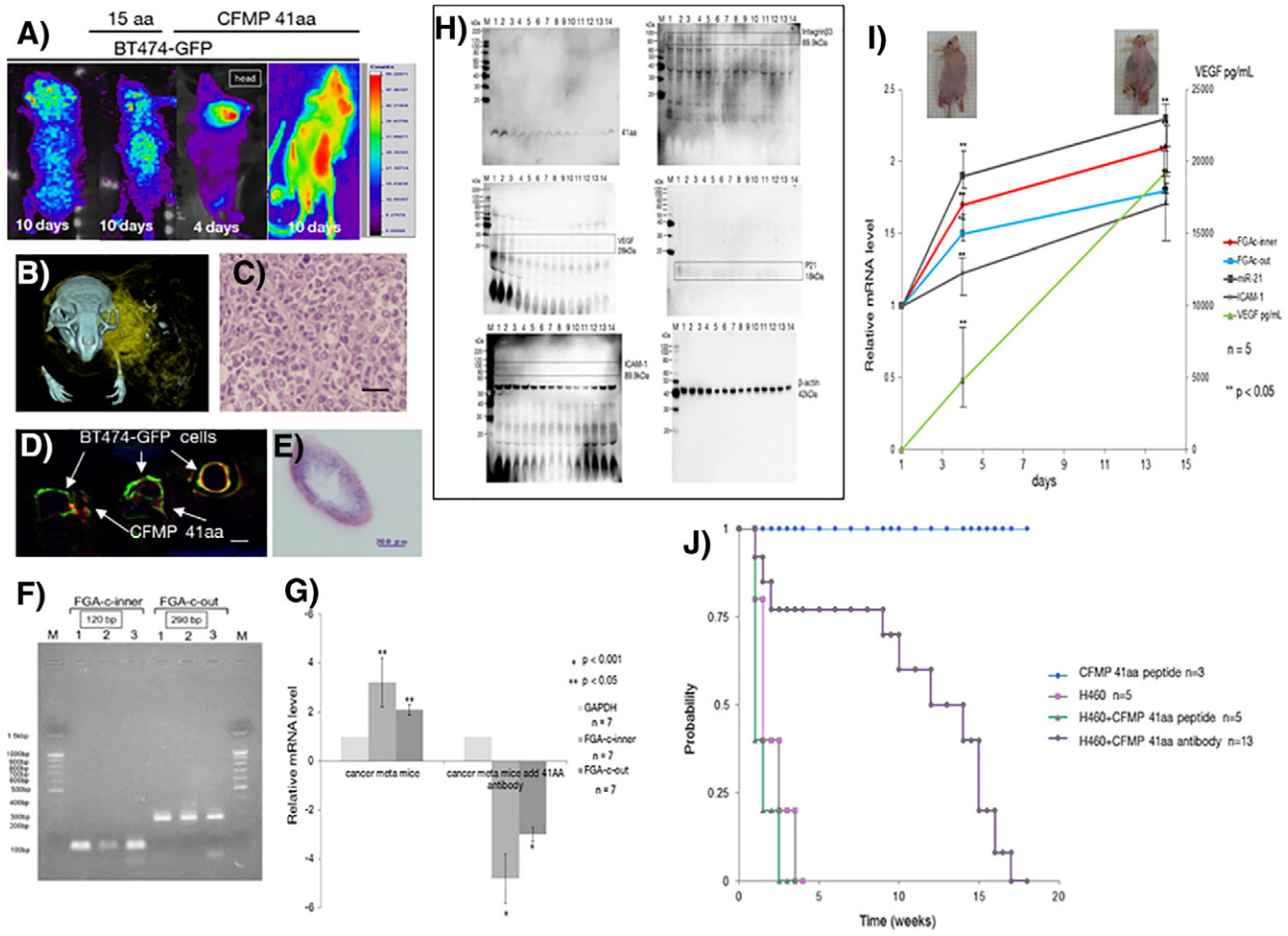

Figure 3. *In vivo* **model of cancer metastasis. (A)** A representative image taken four days after incubating the CFMP peptide with BT474 breast cancer cells and transplanting them into a mouse is shown. BT474 breast cancer cells labeled with GFP and Fluor 594-tagged CFMP (HiLyte Fluor 594 C2 maleimide-CQFTSSTSYNRGDSTFESKSYKMADEAGSEADHEGTHSTKR) were implanted *via* the tail vein in twenty-one female SCID Hairless Outbred (SHO) mice, and fluorescence was observed over time using an Optix MX2 Imager (ART Advanced Research Technologies, Inc., Montreal, Canada). After 4 d, fluorescence appeared in the cranial region. After 10 d, the entire body was fluorescent, and enhanced CFMP visibility was observed. (**B**) 3D–CT imaging confirmed the formation of new blood vessels and bony tissue in a mouse with cancer metastasis. (**C**) Hematoxylin and eosin staining of potentially metastasized tissue revealed the presence of carcinoma. Magnification, 20 ×. (**D**) Co-localization of cancer cells and CFMP. Confocal laser scanning microscopy confirmed the results seen in mice 10 days after injection of the CFMP peptide (see panel A) (Olympus FluoView FV 1000-D; Tokyo, Japan). The peptide was observed in the vascular tissue. Magnification, 10 ×. (**E**) *In situ* hybridization of miR-21. Nuclear Fast Red was used as a comparative stain. Bar: 20 μm. (**F**) PCR primers were designed to amplify regions of the mRNA encoding the CFMP molecule (41 aa), an external sequence (FGAc-out; nucleotides 1683–1972) and the internal sequence (FGAc-inner; nucleotides 1712–1831), and were confirmed to be useful for PCR amplification. (**G**) After injection of an anti-CFMP antibody (7 mg/kg) into mice implanted with cancer cells and CFMP peptides (5 μg/mL; 20 μL/g), the suppression of FGAc expression was examined by real-time PCR. (**H**) Western blotting analysis of SCID mice tissues following injection of CFMP peptide (5 μg/mL; 20 μL/g) and/or H460 cells into the tail vein after 2 weeks. The expression of CFMP, p21, VEGF, and integrin β3 were examined using Western blotting with an anti-CFMP antibody, an anti-p21 antibody (ab16767), an anti-VEGF antibody (TA500289) and an anti-integrin β3 antibody (ab7166), respectively. An anti-beta actin antibody (ab8227) was used as the loading control. *Far left lane:* Molecular weight markers. *Lane 1:* Lung tissue after transplantation with human lung cancer (H460) cells. *Lane 2:* Right lobe of liver tissue after transplantation with H460 cells. *Lane 3:* Left maxillary tumor tissue after transplantation with H460 cells. *Lane 4:* Intestinal tissue after transplantation with H460 cells and CFMP peptide. *Lane 5:* Left lobe of liver tissue after transplantation with H460 cells. *Lane 6:* Left lung tumor tissue after transplantation with H460 cells. *Lanes 7:* Right lung tumor tissue after transplantation with H460 cells. *Lanes 8:* Left lung tumor tissue after transplantation with MNNG/HOS human osteosarcoma cells. *Lane 9:* Culture supernatant derived from H460 cells. *Lane 10:* Culture supernatant derived from MNNG/HOS human osteosarcoma cells. *Lanes 11–14* are vascular tissues from mice implanted with H460 cells and CFMP peptides. (**I**) Quantitative analysis of VEGF values over a time course in SCID mice with metastatic cancer, and corresponding quantitative analysis by real-time PCR of the target. (**J**) All mice received an equivalent volume of cancer cells through their caudal (tail) vein. Thereafter, mice were injected with CFMP peptide (5 μg/mL; 20 μL/g) or an anti-CFMP antibody (7 mg/kg) for survival analyses. *P*-value: 0.0017, hazard ratio (HR) 3.37, 95% confidence interval (CI) 5.66–12.18 (H460 *cf.* H460 + anti-CFMP antibody), *P*-value: 0.073, HR: 1.31, 95% CI 0.64–1.75 (H460 *cf.* H460 + CFMP peptide).

ICAM-1 by qRT-PCR. Transplantation of cancer cells along with CFMP induced higher levels of expression of miR-21 and VEGF, than did cancer cells without the peptide (Figure 3*I*). We also performed a survival analysis to investigate the effect of the anti-CFMP peptide antibody (Supplemental Methods). CFMP by itself had no influence on *in vivo* survival, but in the presence of

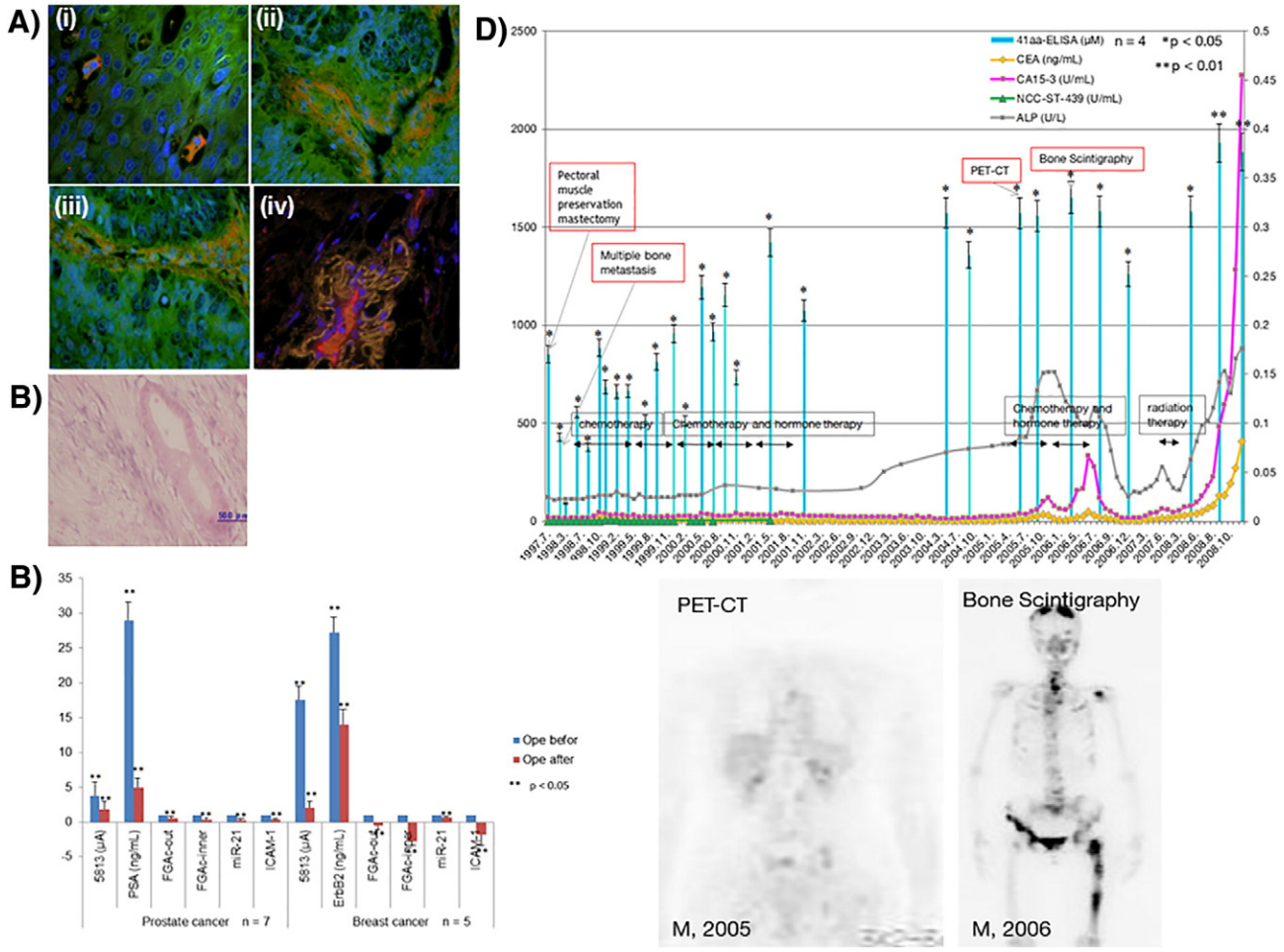

Figure 4. Analysis of clinical samples **(A)** Fluorescent histological staining of cancer tissues using an anti-CFMP antibody (labeled with Alexa Fluor 555), an anti-CD51/CD61 antibody (ab7166) (labeled with Alexa Fluor 488). Nuclei were stained with DAPI (**i**) Metastatic squamous epithelial cancer tissue, male Caucasian, aged 60 years. (**ii**) Metastatic lung cancer tissue, male Caucasian, aged 67 years. (**iii**) Metastatic breast cancer tissue, female Caucasian, aged 58 years. (**iv**) Metastatic ovarian mucinous cystandemo carcinoma tissue, female Caucasian, aged 33 years. All images are at a magnification of 40 ×. Fluorescent staining of metastatic cancer tissue arrays (Z7020073; https://www.biochain.com/search/?fwp_search_bar=Z7020073, Z7020074: https://www.biochain.com/search/?fwp_search_bar=Z7020074, Bio Chain, Institute Inc., Newark, CA, USA) was observed with an Olympus fluorescence microscope BX 50 microscope and analyzed with the Image Pro-plus 4.5 software. (**B**) *In situ* hybridization for CFMP was performed in the metastatic lung cancer tissue of a male Caucasian, aged 60 years. Bar: 50 μm. (**C**) Cancer markers were analyzed before and after tumor extraction from prostate cancer (PSA) and breast cancer (ErbB2) patients. (**D**) A follow-up of breast cancer patients with bone metastasis showed that although CFMP peptide serum levels decreased postoperatively as shown from an ELISA analysis, high CFMP peptide levels were observed 1 year postoperatively. Bone metastasis was confirmed approximately 7 years postoperatively by PET-CT and 8 years postoperatively by bone scintigraphy.

cancer cells the mean mouse survival time was 1 week, compared with 13 weeks for mice injected with the anti-CFMP antibody (Figure 3*J*).

In addition, we also used an anti-CD51/CD61 (platelet glycoprotein GPIIb/IIIa) antibody from a previous study [26,27] to examine its expression using immunofluorescence. Figure 4*A* shows the layout of the primary metastatic cancer tissues (i) metastatic squamous epithelial cancer tissue (ii) metastatic lung cancer tissue, (iii) metastatic breast cancer tissue (iv) metastatic ovarian mucinous cystandemo carcinoma tissue in the arrays we used (Z7020073; https://www.biochain.com/search/?fwp_search_bar=Z7020073, Z7020074: https://www.biochain.com/search/?fwp_search_bar=Z7020074, Bio Chain, Institute Inc., Newark, CA, USA). *In situ* hybridization also revealed that CFMP was detected around the blood vessels of lung-metastasis tissue obtained from Caucasian males with prostate cancer (Figure 4*B*).

A relative quantitative analysis of FGA, miR-21, and ICAM-1 in the blood revealed higher levels of these genes among patients with breast cancer and prostate cancer, both before and after operation. Moreover, CFMP levels, measured by mass spectrometry, as well as measurements of the prostate cancer marker PSA and the breast cancer marker ErbB2, revealed that levels of these markers decreased following tumor excision (Figure 4*C*).

Even if a high level of CFMP peptide is confirmed, a follow-up survey is important for the definitive diagnosis of a cancer metastasis site using image diagnosis. The serum from a 51-year-old female patient who underwent pectoral muscle preservation mastectomy in 1997, due to breast cancer, was examined to detect the appearance of CFMP. Following a request from the PET center of our university hospital, we initiated a prospective study around CFMP in May

2005. At this time, cancer metastasis was not confirmed by PET-CT, but ELISA measurements did confirm a high level of CFMP, and that cancer metastasis was suspected. Therefore, we conducted a retrospective study going back to before the 1997 surgery, which confirmed bone metastasis by bone scintigraphy in October 2005. Although cancer markers (such as CEA, CA15–3, NCC-ST-439, and ALP) had been measured since 1997, they do not enable an early diagnosis like the one that CFMP has made possible (Figure 4*D*).

Discussion

In the present study, we retrospectively investigated the sera obtained from patients who developed bone metastases after liver cancer treatment. We discovered a novel 41-aa peptide, which we refer to as CFMP, in the sera, which was also expressed in cancer metastases, but was absent from osteoclasia in control rheumatoid arthritis samples. Rheumatoid arthritis is a systemic inflammatory disease caused by an immune abnormality, and it primarily targets joints. It is characterized by proliferation in the synovial tissue, which leads to inflammatory synovial granulation and destruction of the Pannus tissue [28]. The mechanism of its onset is suggested to be different from the bone destruction caused by bone metastasis due to cancer. We therefore also examined the expression of CFMP in patients classified according to the U.S. rheumatoid arthritis (ACR) diagnostic criteria, and we found that a class 2 patient and class 4 (severe) patient did not express CFMP.

Therefore, we suggest that this CFMP peptide is specifically related to the mechanism of bone destruction in cancer metastasis and not to the bone destruction in rheumatoid arthritis (Figure S1*A* and Supplemental Mass Data).

We also examined follow-up data in breast cancer patients. We also observed fluctuations in the levels of CEA, CA15–3, NCC-ST-439, ALP, and CFMP by ELISA in the serum (Figure 4*D*) following the removal of breast cancer tissue; bone metastasis was not confirmed in the 3D–CT imaging performed in July 2005. As a result, we measured the serum CFMP levels in these patients. However, since the levels were already 0.32 ± 0.04 μM ($P < .05$), we conducted a prospective study. Bone metastasis was confirmed using diagnostic imaging through bone scintigraphy in July 2006 and we resumed treatment with radiation therapy and chemotherapy. As a result, we examined our previously stored serum, and found that in 1998, the CEA, CA15–3, NCC-ST-439, and ALP markers were within normal levels after surgical removal of breast cancer tissue, but their CFMP peptide levels were 0.09 ± 0.04 μM ($P < .05$), demonstrating an increase. This level of CFMP was not observed in healthy subjects, or patients who did not develop metastasis. A high level of CFMP was observed at the time of bone metastases confirmation by bone scintigraphy; in addition, we observed a decline in the levels of this peptide after treatment initiation.

We also investigated the potential functions of the CFMP peptide. Early detection of breast cancer is relatively easy and the treatment methods are well established, but the question remains as to why after a long period of time (5 to 10 years) do patients then develop bone metastasis? This is puzzling since chemotherapy and radiotherapy are usually clinically effective; one possible explanation is that cancer cells continue to remain in some areas of the body. Therefore, we wanted to understand where these cancer cell depots are located. Because CFMP appears to function by causing the EMT, and therefore is important in the metastases process, we reasoned that the CFMP may be co-localized with cancer cells. As a result, we discovered that CFMP and breast cancer cells were both localized to vascular tissues. Since the CFMP peptide is not expressed in healthy subjects, or in patients with rheumatoid arthritis.

Importantly, the CFMP peptide was present in patients with bone and tumor metastasis, but absent from healthy individuals (Supplemental Mass Data). When it was administered *in vivo*, it caused EMT-related infiltration, angiogenesis, and neovascularization. During EMT, epidermal cells lose their epithelial characteristics and acquire those of mesenchymal cells. Cell-to-cell adhesion is also disrupted, while cell movement and invasive capacity are enhanced. Cells that differentiate into mesenchymal cells promote tissue fibrosis and contribute to the transformation into cancer cells [29]. An miRNA array analysis of migrating cancer cells *in vitro* revealed a high level of expression of miR-199a-3p in mesenchymal stem cells (Table S1), whereas no change in miR-199a-3p was observed in the endothelium of blood vessels found on the membrane (Figure 2*A*).

We concluded that the RGD motif in CFMP was responsible for promoting EMT and cancer invasion. Arginine–glycine–aspartic acid (RGD) is a cell adhesion motif that can aid in the adhesion of cancer cells. It has been identified in fibronectin, osteopontin, and laminin [30,31], and is capable of binding integrin $\alpha_v\beta_3$. This integrin is produced at high levels in the endothelial cells of new blood vessels in cancer tissues; indeed, the radiotracer 18F-galacto-RGD is frequently used as a radioactive drug target for PET imaging of tumors to verify angiogenesis in cancer [32].

CFMP was also shown in the present study to induce the expression of VEGF and ICAM-1 in the vascular tissues of a mouse cancer metastasis model. To confirm the presence of mesenchymal stem cells, western blotting with antibodies to CD90 [33] and p21 was conducted, revealing the expression of p21 in the vascular tissues of these mice. This suggests that CFMP has detected in blood vessels, which is consistent with the finding that human cancer metastasis occurs 5–10 years after the onset of cancer [34]. Based on advances in oncology, primary cancer has become almost controllable. Together with our current findings, this indicates treatment should aim to prevent metastasis to distant organs.

Numerous studies have demonstrated an association between cancers and fibrinogen, a precursor to a blood clotting factor [35–40]. Trousseau's syndrome is a paraneoplastic disorder that was described in 1865, by Armand Trousseau as migratory superficial thrombophlebitis [41]. Previous research reported that a fibrinogen-deficient mouse showed significantly reduced cancer metastases, suggesting that fibrinogen plays an important role in the process of cancer metastasis [41–45]. Moreover, the blood of cancer patients is often in a hypercoagulable state that causes thrombosis [46,47]. In the present study, we observed that CFMP originated from C-terminal region of FGA (576–628 aa) and that it is involved in several important processes, including platelet aggregation to form tumor thrombi around cancer cells, and cancer cell adhesion to the vascular endothelial beds of metastasis target organs, thereby facilitating extravascular invasion through fibrinogen receptors and metastasis formation; to our knowledge, these mechanisms have not previously been elucidated. Fibrinogen is known to promote the adhesion of leukocytes to vascular endothelial cells *via* an interaction with ICAM-1 and to further mediate migration across the vascular endothelium [48]. However, fibrinogen itself has no physiological activity and is degraded *in vivo* into various fragments by proteases such as thrombin. Consequently, it is unclear why this novel peptide is cleaved at this specific site.

Ohga et al. [49], previously reported that highly metastatic tumor-derived vascular endothelial cells have stem cell-like properties, which might explain our finding that CFMP exists in the blood vessels of patients with metastatic cancer, causes EMT, and moves towards the mesenchymal stem cells. In our *in vitro* model of metastatic invasion, miR-199-3a expression was detected in the membrane between the cancer cells and the upper cell layer, whereas miR-21 expression was observed in the 3D gel. This experiment also revealed that plasmin activity was decreased, whereas p21 was up-regulated, when H460 cells and vascular endothelial cells were co-cultured in the presence of CFMP, with no changes being observed in the absence of the peptide. This was presumably because in the period following excision of the primary tumor, during which a small number of residual cancer cells generate new blood vessels and were hidden in thrombi. We also found that tumor cells were confined to a net-like structure within the metastatic tissue and were obscured inside the blood vessels or at the vessel wall.

Two variants of FGA result from alternative splicing. The CFMP 41-aa sequence identified in this study is present in both isoforms, but is C-terminally located only in the shorter isoform 2 (P02671–2). In the canonical isoform 1 (P02671–1), which is considerably longer that isoform 2, the 41-aa sequence is not located near the C-terminus (see http://www.uniprot.org/uniprot/P02671#sequences). Our present findings suggest that the FGA precursor fragment of the C-terminal region is strongly involved in cancer metastasis, perhaps through the cross-linking of cancer cells and platelets, as well as through the formation of neoplasm thrombi. Following surgical removal of the primary tumor in our metastatic patients, we observed a reduced expression of cancer markers as well as CFMP, suggesting that blocking the peptide within cancer cells could be used for the early identification of cancer metastasis. This would be of benefit in novel drug development. We also anticipate the development of biomarkers based on CFMP and PET-CT tracers for the diagnosis of early-stage metastases after the remission of original cancers [50]. These future developments could help clinicians and researchers to determine likely metastatic sites prior to the emergence of symptoms. This would enable earlier [51,52], more specific, and sensitive treatment of metastatic liver cancer to be achieved compared with existing methods. The findings of our study also suggest that the RGD peptide in the fibrinogen alpha chain could cause Trousseau's syndrome.

Contributions

M.T., M.T., and M.S. designed the study; M.S., K.M., M.T., M.T., T.F., H.Y., and K.N. collected study samples and data; M.T., K.Y., S.M., N.A., H.U., and Y.K. processed tumor samples and performed the proteomics analysis; M.T., M.T., M.S., and N.A. analyzed the study data; and M.T. wrote the manuscript.

Competing Interests

The authors declare that they have no competing interests.

Funding

No benefits in any form have been received or will be received from a commercial party related directly or indirectly to the subject of this article. Funds were received in total or partial support of the research or clinical study presented in this article. The funding sources were a research grant for Cabinet Office Special Coordination Funds for Promoting Science and Technology and Welfare Sciences and the Japan Society for the Promotion of Science Kakenhi (nos. 16,390,445 and 19,591,741).

Transcript profiling

Microarray data are available in the Gene Expression Omnibus (GEO) database (http://www.ncbi.nlm.nih.gov/geo/) under accession number GSE43105.

Acknowledgments

We would like to acknowledge the individuals and families that participated in this research. We dedicate this article to the late emeritus professor Akio Nomoto (Department of Microbiology, Graduate School of Medicine, University of Tokyo). We thank K. Fujii (Kurume General Hospital), R. Hachisu (Hokkaido System Science Co.), E. Majima (ProteNova Co.), H. Saito (Charles River Laboratories Japan, Inc.), K. Gondou, and H. Rakumura (Kurume Research Park Co.) for their helpful comments.

Appendix A. Supplementary data

Supplementary data to this article can be found online at https://doi.org/10.1016/j.tranon.2017.10.001.

References

[1] http://globocan.iarc.fr/Pages/fact_sheets_cancer.aspx.
[2] Sata M, Ide T, Akiyoshi F, Fukuizumi K, Noguchi S, Shirachi M, Sasaki M, Uchimura Y, Suzuki H, and Tanikawa K (1997). Effects of interferon alpha 2a on incidence of hepatocellular carcinoma in chronic active hepatitis without cirrhosis. Hepatitis Treatment Study Group. *Kurume Med J* **44**, 171–177.
[3] Miyajima I, Sata M, Kumashiro R, Uchimura Y, Ide T, Suzuki H, and Tanikawa K (1998). The incidence of hepatocellular carcinoma in patients with chronic hepatitis C after interferon treatment. *Oncol Rep* **5**, 201–204.
[4] Nagao Y, Tanaka K, Kobayashi K, Kumashiro R, and Sata M (2004). Analysis of approach to therapy for chronic liver disease in an HCV hyperendemic area of Japan. *Hepatol Res* **28**, 30–35.
[5] Shimauchi Y, Tanaka M, Kuromatsu R, Ogata R, Tateishi Y, Itano S, Ono N, Yutani S, Nagamatsu H, and Matsugaki S, et al (2000). A simultaneous monitoring of Lens culinaris agglutinin A-reactive alpha-fetoprotein and des-gamma-carboxy prothrombin as an early diagnosis of hepatocellular carcinoma in the follow-up of cirrhotic patients. *Oncol Rep* **7**, 249–256.
[6] Wu JS, Wong R, Johnston M, Bezjak A, Whelan T, and Cancer Care Ontario Practice Guidelines Initiative Supportive Care Group (2003). Meta-analysis of dose-fractionation radiotherapy trials for the palliation of painful bone metastases. *Int J Radiat Oncol Biol Phys* **55**, 594–605.
[7] Meeuse JJ, van der Linden YM, van Tienhoven G, Gans RO, Leer JW, Reyners AK, and Dutch Bone Metastasis Study Group (2010). Efficacy of radiotherapy for painful bone metastases during the last 12 weeks of life: results from the Dutch Bone Metastasis Study. *Cancer* **116**, 2716–2725.
[8] https://www.env.go.jp/en/laws/nature/act_wm_animals.pdf.
[9] Flecknell PA (2009). Laboratory Animal Anaesthesia. 3. London: Academic Press; 2009.
[10] Wallace J (2000). Humane endpoints and cancer research. *ILAR J* **41**, 87–93.
[11] Mahler M, Berard M, Feinstein R, Gallagher A, Illgen B, Pritchett K, and Raspa M (2014). FELASA recommendations for the health monitoring of mouse, rat, hamster, guinea pig and rabbit colonies in breeding and experimental units. *Lab Anim* **48**, 178–192.
[12] Pritchett-Corning KR, Prins JB, Feinstein R, Goodwin J, Nicklas W, Riley L, Federation of Laboratory Animal Science AssociationsAmerican Association for Laboratory Animal Science (2014). AALAS/FELASA Working Group on Health Monitoring of rodents for animal transfer. *J Am Assoc Lab Anim Sci* **53**, 633–640.
[13] http://www.iclasmonic.jp/en/index.html.
[14] http://www.jsh.or.jp/English/examination_en.
[15] Marx V (2013). Targeted proteomics. *Nat Methods* **10**, 19–22.
[16] Abdelhamid HN, Chen ZY, and Wu HF (2017). Surface tuning laser desorption/ionization mass spectrometry (STLDI-MS) for the analysis of small molecules using quantum dots. *Anal Bioanal Chem* **409**, 4943–4950.

[17] Tanase CP, Codrici E, Popescu ID, Mihai S, Enciu AM, Necula LG, Preda A, Ismail G, and Albulescu R (2017). Prostate cancer proteomics: Current trends and future perspectives for biomarker discovery. *Oncotarget* **8**, 18497–18512.

[18] Boja ES, Fehniger TE, Baker MS, Marko-Varga G, and Rodriguez H (2014). Analytical validation considerations of multiplex mass-spectrometry-based proteomic platforms for measuring protein biomarkers. *J Proteome Res* **13**, 5325–5332.

[19] Kanki Y, Kohro T, Jiang S, Tsutsumi S, Mimura I, Suehiro J, Wada Y, Ohta Y, Ihara S, and Iwanari H, et al (2011). Epigenetically coordinated GATA2 binding is necessary for endothelium-specific endomucin expression. *EMBO J* **30**, 2582–2595.

[20] Radisky ES and Radisky DC (2010). Matrix metalloproteinase-induced epithelial-mesenchymal transition in breast cancer. *J Mammary Gland Biol Neoplasia* **15**, 201–212.

[21] Partridge NC, Walling HW, Bloch SR, Omura TH, Chan PT, Pearman AT, and Chou WY (1996). The regulation and regulatory role of collagenase in bone. *Crit Rev Eukaryot Gene Expr* **6**, 15–27.

[22] Hess J, Porte D, Munz C, and Angel P (2001). AP-1 and Cbfa/runt physically interact and regulate parathyroid hormone-dependent MMP13 expression in osteoblasts through a new osteoblast-specific element 2/AP-1 composite element. *J Biol Chem* **276**, 20029–20038.

[23] Hedbäck N, Jensen DH, Specht L, Fiehn AM, Therkildsen MH, Friis-Hansen L, Dabelsteen E, and von Buchwald C (2014). MiR-21 Expression in the tumor stroma of oral squamous cell carcinoma: an independent biomarker of disease free survival. *PLoS One* **9**, e95193.

[24] Zhang Y, Pan T, Zhong X, and Cheng C (2014). Nicotine up-regulates microRNA-21 and promotes TGF-β-dependent epithelial-mesenchymal transition of esophageal cancer cells. *Tumour Biol* **35**, 7063–7072.

[25] Mussnich P, D'Angelo D, Leone V, Croce CM, and Fusco A (2013). The High Mobility Group A proteins contribute to thyroid cell transformation by regulating miR-603 and miR-10b expression. *Mol Oncol* **7**, 531–542.

[26] Offermanns S, Toombs CF, Hu TH, and Simon MI (1997). Defective platelet activation in G alpha(q)-deficient mice. *Nature* **389**, 183–186.

[27] Podolnikova NP, Yakubenko VP, Volkov GL, Plow EF, and Ugarova TP (2003). Identification of a novel binding site for platelet integrins alpha IIb beta 3 (GPIIbIIIa) and alpha 5 beta 1 in the gamma C-domain of fibrinogen. *J Biol Chem* **278**, 32251–32258.

[28] Kirwan J, Byron M, and Watt I (2001). The relationship between soft tissue swelling, joint space narrowing and erosive damage in hand X-rays of patients with rheumatoid arthritis. *Rheumatology (Oxford)* **40**, 297–301.

[29] Shirakihara T, Horiguchi K, Miyazawa K, Ehata S, Shibata T, Morita L, Miyazono K, and Saitoh M (2011). TGF-β regulates isoform switching of FGF receptors and epithelial-mesenchymal transition. *EMBO J* **30**, 783–795.

[30] Ruoslahti E and Pierschbacher MD (1987). New perspectives in cell adhesion: RGD and integrins. *Science* **238**, 491–497.

[31] Pierschbacher MD and Ruoslahti E (1984). Cell attachment activity of fibronectin can be duplicated by small synthetic fragments of the molecule. *Nature* **309**, 30–33.

[32] Liu S (2009). Radiolabeled cyclic RGD peptides as integrin alpha(v)beta(3)-targeted radiotracers: maximizing binding affinity via bivalency. *Bioconjug Chem* **20**, 2199–2213.

[33] Dominici M, Le Blanc K, Mueller I, Slaper-Cortenbach I, Marini F, Krause D, Deans R, Keating A, Prockop DJ, and Horwitz E (2006). Minimal criteria for defining multipotent mesenchymal stromal cells. The International Society for Cellular Therapy position statement. *Cytotherapy* **8**, 315–317.

[34] Kurtz JM, Spitalier JM, and Amalric R (1983). Late breast recurrence after lumpectomy and irradiation. *Int J Radiat Oncol Biol Phys* **9**, 1191–1194.

[35] Yamashita H, Kitayama J, Kanno N, Yatomi Y, and Nagawa H, et al (2006). Hyperfibrinogenemia is associated with lymphatic as well as hematogenous metastasis and worse clinical outcome in T2 gastric cancer. *BMC Cancer* **6**, 147.

[36] Ikeda M, Furukawa H, Imamura H, Shimizu J, Ishida H, Masutani S, Tatsuta M, and Satomi T (2002). Poor prognosis associated with thrombocytosis in patients with gastric cancer. *Ann Surg Oncol* **9**, 287–291.

[37] Gouin-Thibault I, Achkar A, and Samama MM (2001). The thrombophilic state in cancer patients. *Acta Haematol* **106**, 33–42.

[38] Modrau IL, Iversen LL, and Thorlacius-Ussing OO (2001). Hemostatic alterations in patients with benign and malignant colorectal disease during major abdominal surgery. *Thromb Res* **104**, 309–315.

[39] Douketis JD, Kearon C, Bates S, Duku EK, and Ginsberg JS, et al (1998). Risk of fatal pulmonary embolism in patients with treated venous thromboembolism. *JAMA* **279**, 458–462.

[40] Palumbo JS, Potter JM, Kaplan LS, Talmage K, Jackson DG, and Degen JL (2002). Spontaneous hematogenous and lymphatic metastasis, but not primary tumor growth or angiogenesis, is diminished in fibrinogen-deficient mice. *Cancer Res* **62**, 6966–6972.

[41] Trousseau A (1865). Phlegmasia alba dolens. In: Bailliere JB, editor. Clinique Medicale de l'Hotel-Dieu de Paris, 3. , , 2nd ed.; 1865. p. 654–712.

[42] Palumbo JS, Kombrinck KW, Drew AF, Grimes TS, Kiser JH, Degen JL, and Bugge TH (2000). Fibrinogen is an important determinant of the metastatic potential of circulating tumor cells. *Blood* **96**, 3302–3309.

[43] Biggerstaff JP, Seth N, Amirkhosravi A, Amaya M, Fogarty S, Meyer TV, Siddiqui F, and Francis JL, et al (1999). Soluble fibrin augments platelet/tumor cell adherence in vitro and in vivo, and enhances experimental metastasis. *Clin Exp Metastasis* **17**, 723–730.

[44] Dvorak HF, Senger DR, and Dvorak AM (1983). Fibrin as a component of the tumor stroma: origins and biological significance. *Cancer Metastasis Rev* **2**, 41–73.

[45] Hu C, Chen R, Chen W, Pang W, Xue X, Zhu G, and Shen X (2014). Thrombocytosis is a significant indictor of hypercoagulability, prognosis and recurrence in gastric cancer. *Exp Ther Med* **8**, 125–132.

[46] Pedersen LM and Milman N (1996). Prognostic significance of thrombocytosis in patients with primary lung cancer. *Eur Respir J* **9**, 1826–1830.

[47] Languino LR, Plescia J, Duperray A, Brian AA, Plow EF, Geltosky JE, and Altieri DC (1993). Fibrinogen mediates leukocyte adhesion to vascular endothelium through an ICAM-1-dependent pathway. *Cell* **73**, 1423–1434.

[48] Languino LR, Duperray A, Joganic KJ, Fornaro M, Thornton GB, and Altieri DC, et al (1995). Regulation of leukocyte-endothelium interaction and leukocyte transendothelial migration by intercellular adhesion molecule 1-fibrinogen recognition. *Proc Natl Acad Sci U S A* **92**, 1505–1509.

[49] Ohga N, Ishikawa S, Maishi N, Akiyama K, Hida Y, Kawamoto T, Sadamoto Y, Osawa T, Yamamoto K, and Kondoh M, et al (2012). Heterogeneity of tumor endothelial cells: comparison between tumor endothelial cells isolated from high- and low-metastatic tumors. *Am J Pathol* **180**, 1294–1307.

[50] Blattmann C, Oertel S, Thiemann M, Dittmar A, Roth E, Kulozik AE, Ehemann V, Weichert W, Huber PE, and Stenzinger A, et al (2015). Histone deacetylase inhibition sensitizes osteosarcoma to heavy ion radiotherapy. *Radiat Oncol* **10**, 146.

[51] Agrawal K, Marafi F, Gnanasegaran G, van der Wall H, and Fogelman I (2015). Pitfalls and limitations of radionuclide planar and hybrid bone imaging. *Semin Nucl Med* **45**, 347–372.

[52] Aung W, Jin ZH, Furukawa T, Claron M, Boturyn D, Sogawa C, Tsuji AB, Wakizaka H, Fukumura T, and Fujibayashi Y, et al (2013). Micro-positron emission tomography/contrast-enhanced computed tomography imaging of orthotopic pancreatic tumor-bearing mice using the $\alpha v\beta_3$ integrin tracer ^{64}Cu-labeled cyclam-RAFT-c(-RGDfK-)$_4$. *Mol Imaging* **12**, 376–387.